THE INVESTIGATION OF AN Al-Zr-Ti ALLOY PREPARED BY SPARK PLASMA SINTERING OF ATOMIZED POWDER

MOLNÁROVÁ Orsolya[1*], MÁLEK Přemysl[1], LUKÁČ František[2], CHRÁSKA Tomáš[2], CINERT Jakub[2]

[1]*Charles University in Prague, Czech Republic, EU, *mopersze@gmail.com*
[2]*Institute of Plasma Physics of the CAS, Prague, Czech Republic, EU*

Abstract

The microstructure and mechanical properties of a powder metallurgical Al-Zr-Ti alloy was studied. Fine powder with a typical size below 50 μm was prepared by gas atomization. The smallest powder particles with a diameter below 10 μm exhibited a segregation free microstructure. Larger droplets were found to contain intermetallic particles rich in Zr and Ti. The gas atomized powder was consolidated by spark plasma sintering (SPS) at various temperatures ranging from 450 to 550 °C. During SPS the materials microstructure remained nearly unchanged and a fine grain size between 2 and 3 μm was observed. All SPS samples exhibited a microhardness of around 90 HV. The annealing (1 h, 500 °C) of the sample sintered at the highest temperature (550 °C) resulted in a decrease of microhardness to 75 HV as a result of changes in the phase composition, the fine grain size was retained. Natural aging at room temperature was not observed.

Keywords: Gas atomization, spark plasma sintering, high strength alloy, thermal stability

1. INTRODUCTION

The development of high strength Al-based alloys which would be stable at elevated temperatures is a long-term goal of material research. The main criteria for the alloying elements capable to produce such Al-based alloys are as follows: (a) The alloying element should form precipitates of an intermetallic compound with Al which will enhance the strength. (b) The alloying element should have a very low solid solubility up to high temperatures which prevents the strengthening particles from dissolution. (c) The alloying element should have a low diffusivity in Al matrix and the strengthening precipitates should have a low lattice mismatch with the Al matrix. In this case, the Ostwald ripening of precipitates can be reduced. By introduction of dense, homogeneously distributed, fine and coarsening resistant precipitates into the aluminum matrix a potential candidate for a high strength high temperature Al-based alloy can be produced.

The Al-Zr system containing precipitates of the Al_3Zr intermetallic compound has a high potential as a thermally stable high strength aluminum alloy. The formation of the equilibrium tetragonal Al_3Zr (structure type DO_{23}) phase is preceded by the formation of a metastable cubic $L1_2$ phase. This metastable phase exhibits a higher resistance to coarsening, especially because of a very similar structure to the Al-based matrix. The transformation of the high symmetry cubic $L1_2$ structure to the tetragonal DO_{23} one occurs at relatively high temperatures with prolonged exposure [1]. The stability of the cubic phase can be further increased by alloying with other elements (e.g. Ti, Hf, V) substituting for Zr atoms in the $L1_2$ lattice and reducing the lattice mismatch to Al-based matrix [2, 3]. It was shown in [4] that the lattice mismatch of the metastable $Al_3(Zr_{0.7}Ti_{0.3})$ phase is practically zero and these particles should be extremely resistant to coarsening.

Materials strength can be further increased by a grain size reduction. Materials with a fine grain size can be prepared using rapid solidification methods, e.g. by gas atomization. High cooling rates lead to a fine microstructure, extension of solid solubility, formation of non-equilibrium phases, all enhancing the strength of powders [5]. A suitable consolidation method which preserves all these benefits of gas atomization has to be chosen. Spark plasma sintering (SPS) combines uniaxial pressure with heating by low voltage DC current

flowing through the sample [6]. In this process, high current densities and large Joule heat are observed primarily at the powder surfaces, the powder interiors are nearly unaffected. Due to high heating rates, relatively low sintering temperatures and short thermal exposure of sintered powder material undesirable processes connected with solute reorganization and recrystallization can be strongly limited.

The general aim of our study is to produce a thermally stable high strength aluminum alloy. As a first step, a combination of gas atomization and SPS was used at the Al-Zr-Ti alloy. Microstructure and microhardness of both powders and SPS compacts were investigated along with thermal stability of the sintered material.

2. EXPERIMENTAL

The nitrogen atomized Al-Zr-Ti powder supplied by Nanoval GmbH & Co. KG, Berlin was sieved down to 50 µm. The resulting average powder particle size was 20 µm. According to the producer, the alloy contains 2.6 wt.% of Zr and 0.7 wt.% of Ti (the corresponding Zr : Ti ratio in at. % is 65 : 35). The atomized powder was compacted by SPS using FCT SPS-HP25 (FCT Systeme GmbH). During consolidation, the samples were free heated up to 400°C, the sintering temperature (450, 475, 500, 525, 550 °C) was reached with a heating rate of 25°C/min. Uniaxial pressure of 80 MPa was applied to the powder during SPS which was increased simultaneously with temperature. The holding time was 4 min.

Samples morphology and microstructure were investigated by scanning electron microscopy (SEM) using FEI Quanta 200F microscope equipped with field emission cathode (FEG). Chemical composition was studied by energy dispersive X-ray spectroscopy (EDS). The grain size and grain orientations were analysed using electron backscattered diffraction (EBSD). Microstructural investigation of compacts was performed on samples cut parallel to the direction of the applied stress during SPS.

Phase composition was investigated by X-ray diffraction (XRD). Quantitative Rietveld analysis was performed in TOPAS V5, aiming at the determination of weight fractions of present phases. For details see [7].

Material strength was characterised by Vickers microhardness measured using a Qness Q10A+ microhardness tester. The load of 10 g was applied at the powder material. At least 15 different powder particles were measured. The load of 50 g was applied at compact samples. To study the material homogeneity an area of 4x4 mm^2 was tested automatically with a distance between indents of 200 µm.

3. RESULTS

Gas atomization resulted in spherical powder particles (**Figure 1a**). Numerous very small particles (below 10 µm) exhibit a segregation free microstructure (see arrow). The microstructure of coarser particles is mostly cellular, rarely dendritic-like cellular, with the cell size of about 2 µm (**Figure 1b**).

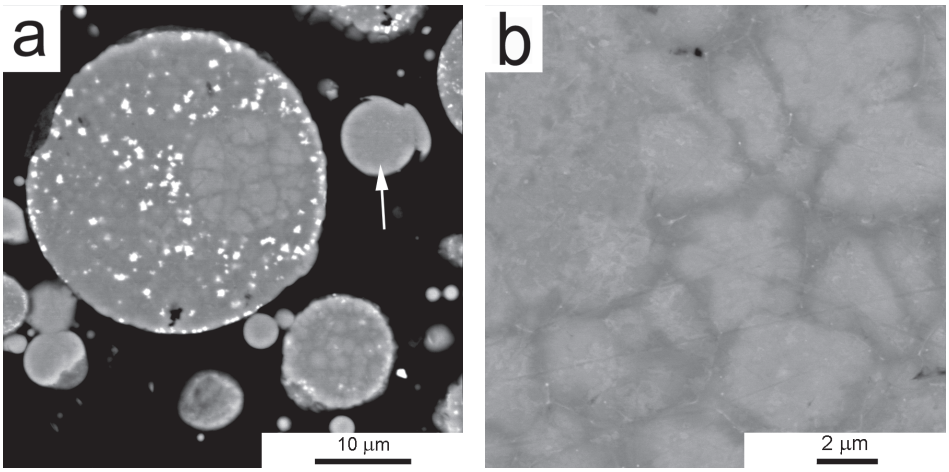

Figure 1 Gas atomized powder particles a) morphology and microstructure, b) detail, BSE

Especially the largest particles contain relatively coarse precipitates. EDS measurement revealed that these precipitates contain both Zr and Ti (**Figure 2**). The investigation of the distribution of alloying elements within the cell microstructure revealed that the intercellular regions are depleted of Zr and Ti.

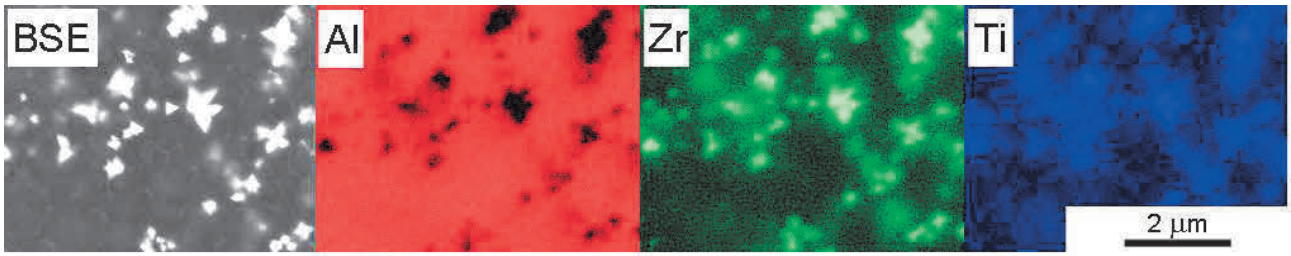

Figure 2 Elements distribution in a large gas atomized particle, BSE and the corresponding EDS maps

EBSD investigation showed the fine grain structure of atomized powders. An average grain size between 2 and 3 μm was evaluated from measurements performed on 10 randomly selected powder particles. **Figure 3** shows a representative powder particle in BSE contrast along with the orientation image map of this particle.

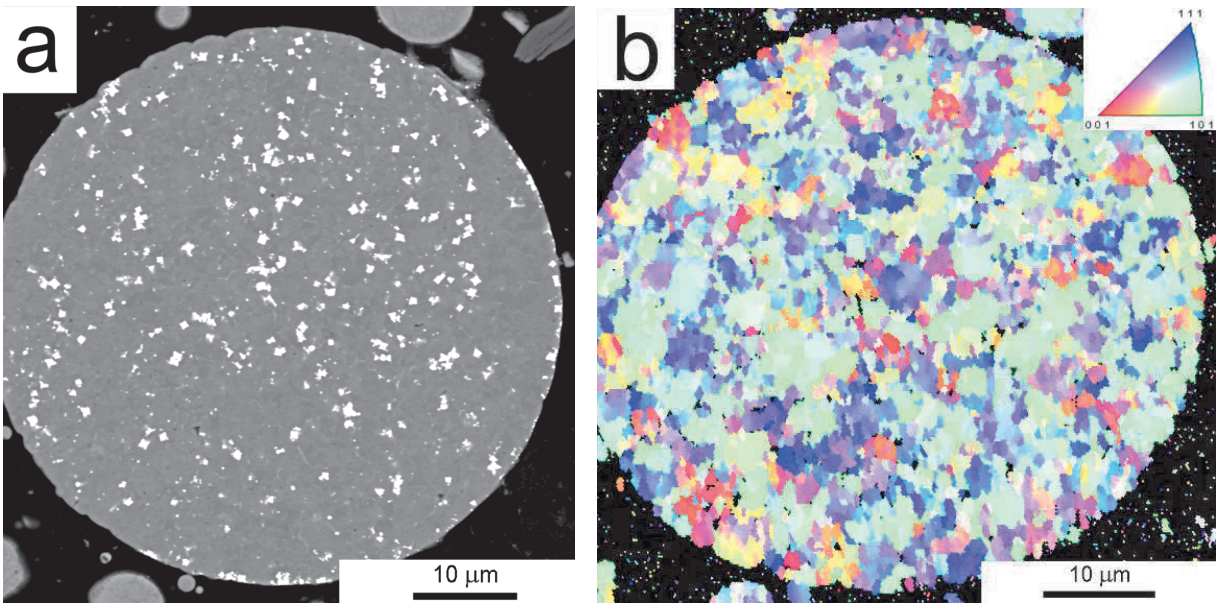

Figure 3 A gas atomized powder particle a) BSE contrast, b) the corresponding EBSD micrograph

Powders were compacted by SPS at various temperatures. Large pores (see arrows) were observed after SPS at 450 °C, a fully dense compact was obtained only at the highest sintering temperature of 550 °C (**Figure 4**). The internal microstructure of SPS compacts is similar to that of the powder material. The former powder particles are still recognisable. The largest powder particles were found to be slightly deformed during SPS, the smaller powder particles retained their spherical shape.

SPS compacts contain both larger (1 μm) precipitates present already in the powder and smaller, needle shaped precipitates. XRD measurements revealed that these precipitates are formed by the $Al_3(Zr,Ti)$ phase both with the $L1_2$ and DO_{23} structure. The total weight fraction of the $Al_3(Zr,Ti)$ phase increased slightly with increasing sintering temperature. Simultaneously, the metastable $L1_2$ phase was gradually replaced by the stable DO_{23} phase (3.1 wt.% of the $L1_2$ phase after sintering at 450 °C, 1.8 wt.% of the $L1_2$ phase and 1.6 wt.% of the DO_{23} phase after sintering at 550 °C).

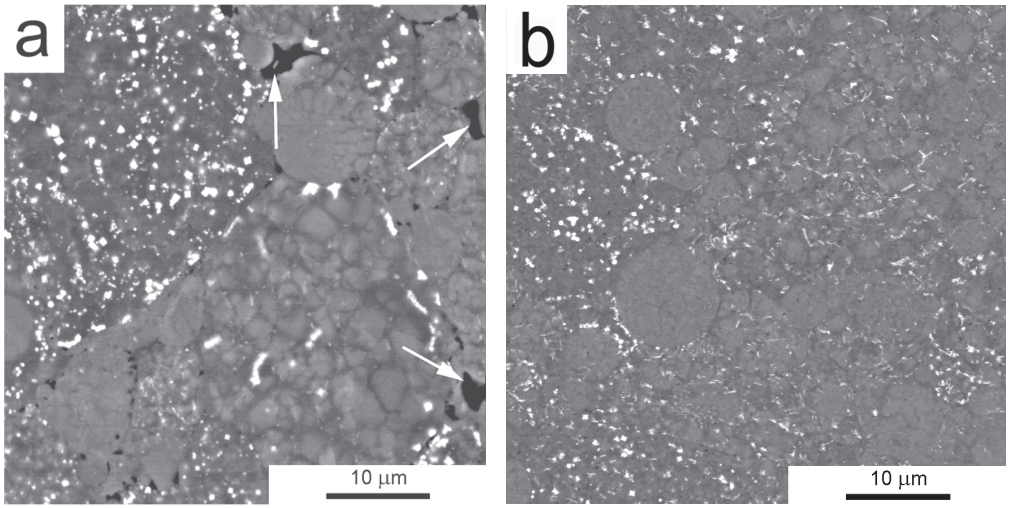

Figure 4 Microstructure of compacts prepared by SPS at a) 450 °C, b) 550 °C, BSE contrast

The mean grain size determined using EBSD mapping was found between 2 and 3 µm in all compacts independently of the SPS temperature. **Figure 5** compares compacts microstructure in BSE contrast with its grain structure presented by an orientation map. The fraction of high-angle boundaries was stated to be 87%. The original smallest powder particles seem to be without precipitates and mostly monocrystalline, whereas the original largest powder particles are polycrystalline.

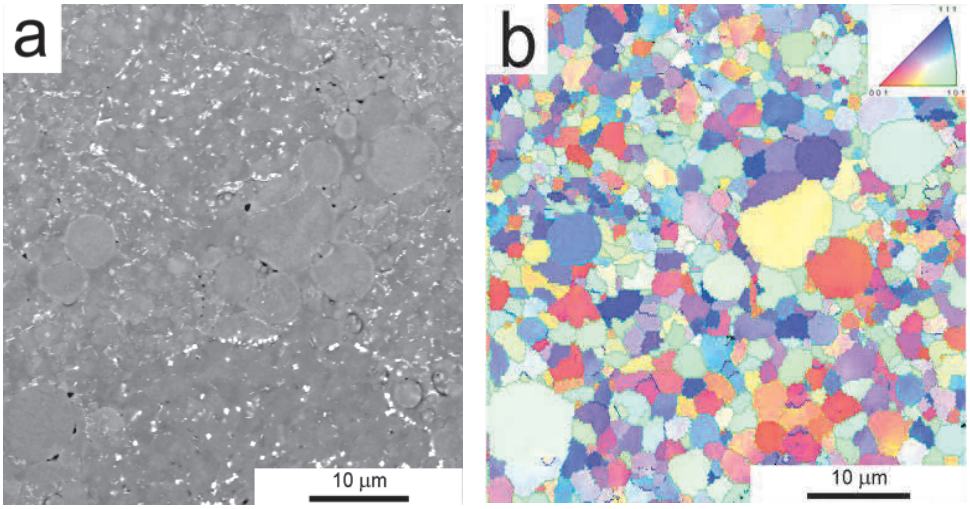

Figure 5 Microstructure of the compact sintered at 550 °C, a) BSE contrast, b) the corresponding EBSD micrograph

The mechanical properties of both powders and SPS compacts were tested by microhardness measurement. Whereas powders exhibited a relatively low microhardness of (49 ± 12) HV, the microhardness of SPS compacts was (90 ± 8) HV, nearly independent of the temperature of sintering (within the standard deviation).

The thermal stability was studied on the compact sintered at 550 °C. This compact was annealed at 500 °C for 1 h followed by water quenching and then stored at room temperature for a long time. Its microstructure was similar to that of the non-annealed material and EBSD mapping revealed no grain coarsening (within the standard deviation). XRD measurements showed an increase in precipitates weight fraction due to heat treatment. A partial transition from the $L1_2$ to the DO_{23} modification of the $Al_3(Zr,Ti)$ phase also confirmed (1.7 wt.% of the $L1_2$ phase and 1.9 wt.% of the DO_{23} phase after 1 h annealing at 500 °C).

Samples microhardness was found to decrease slightly to (76 ± 7) HV after annealing at 500 °C. This microhardness does not change during a following long term stay at room temperature.

4. DISCUSSION

The Al-Zr-Ti alloy should deduce its high strength from a dense distribution of fine $Al_3(Zr_xTi_{1-x})$ precipitates. As showed in [8], chill casting is not capable to produce such a microstructure because of a massive formation of coarse primary particles during solidification. On the other site, rapid solidification was reported to suppress formation of these coarse primary particles and to refine materials microstructure [5]. The cooling rates up to 10^6 K/s applied in the melt spinning of the Al-Zr-Ti alloy with various contents of Zr and Ti resulted in the production of supersaturated ribbons exhibiting fine microstructure. The following thermal treatment led to the precipitation of fine $L1_2$ $Al_3(Zr,Ti)$ particles arranged frequently into fans. The main drawbacks of melt spinning method are the microstructure and phase composition inhomogeneity in the direction perpendicular to the ribbon plane and the difficulty of consolidation process [9, 10].

The cooling rates applied in the gas atomization process are generally slower and vary especially with the size of powder droplets. In coarser particles, a gradient of cooling rate from the surface to the centre of droplets can introduce further microstructural and phase composition inhomogeneity. The investigation of the same alloy with significantly coarser powder particles (sieved below 100 μm) revealed a cellular or dendritic microstructure [11]. In our material, the very small powder particles are even segregation free. In coarser powder particles, the distribution of alloying elements within the cell structure corresponds to the peritectic type of phase diagram - the intercellular regions are depleted of alloying elements. Relatively coarse primary particles of the $Al_3(Zr,Ti)$ phase were observed especially in coarse powder particles. The formation of these primary particles can be supported by the presence of Ti. Whereas a high supersaturation can be achieved in binary Al-Zr system (8.6 wt.% of Zr can be dissolved in the Al matrix [11]), the addition of Ti resulted in the formation of coarse primary $Al_3(Zr,Ti)$ particles even in the melt spun ribbons [9]. The relatively low microhardness found in the powder material can be explained by the fact that the measurements were performed only in the largest particles containing coarse primary particles which do not contribute significantly to the strength.

SPS of powder particles led to dense compacts, however a full density was reached only at the highest sintering temperature. Comparing the microstructure of different compacts, densification occurred by a flow of fine particles into voids between coarse ones and concurrent deformation of large powder particles in accordance with [13]. The short thermal exposure during SPS minimized the influence of sintering on the powders original microstructure. Therefore, former powder particles are still recognisable in compacts and the fine grain structure was preserved. On the other side, hot extrusion used for the consolidation of powder material in [11] resulted in a complete destruction of the original microstructure and its replacement by a hot-worked microstructure.

Changes in the weight fraction and structure of the strengthening $Al_3(Zr,Ti)$ phases occurred during SPS. Similar trends were observed in [14] after a long high temperature exposure. Similar replacement of the metastable $L1_2$ by the stable DO_{23} modification was also observed in the cast Al-0.1Zr or Al-0.1Zr-0.1Ti alloy [15]. Heat exposure up to 450 °C caused no transition, whereas structural transformation started at 525 °C after extended aging times, predominantly on dislocations due to the faster pipe diffusion.

In contrast to the materials high thermal stability the compacts exhibited a relatively low microhardness, which is comparable to the value 98 HV, obtained for similar as melt-spun Al-Zr-Ti alloy [9]. Microhardness further decreased during heat treatment. Since materials grain size was found not to be altered by the heat exposure, this drop in microhardness should be connected with precipitate evolution. As showed in [9] and [15] the

microhardness of Al-Zr-Ti alloys decreases after heat treatment at 500 °C due to formation of coarser DO_{23} $Al_3(Zr,Ti)$ phase.

In order to produce a high strength material on the base of this Al-Zr-Ti alloy, a remarkable decrease in grain size and suppression of coarse precipitates are necessary. Both effects can be achieved by mechanical milling. Choosing a proper consolidation method with minimal influence on microstructure, like SPS, favourable properties from milling can be retained. Further experiments will therefore focus on mechanical milling of atomized Al-Zr-Ti alloy, followed by sintering to bulk samples by SPS.

5. CONCLUSION

The Al-Zr-Ti alloy prepared by gas atomization and spark plasma sintering was studied. Gas atomization resulted in spherical powder particles with predominantly cellular microstructure. The intercellular regions were depleted of Zr and Ti. Coarse primary precipitates were found especially in larger powder particles. SPS led to full density compact only at the highest temperature. Sintering at increased temperatures led to formation of the stable DO_{23} modification of the $Al_3(Zr,Ti)$ phase. The fine grain size was retained after SPS and also after further annealing at 500 °C.

ACKNOWLEDGEMENTS

This work was financially supported by the grant GACR 15-15609S.O.M. is grateful for financial support from the grant SVV-2017-260213.

REFERENCES

[1] HUANG, Y., LANGDON, T. G. Advances in ultrafine-grained materials. *Materials Today*, 2013, vol. 16, no. 3, pp. 85-93.

[2] FINE, M. E. Stability and coarsening of dispersoids in aluminum alloys. In: *Dispersion Strengthened Aluminum Alloys*. Warrendale, PA: TMS; 1988, pp. 103-121.

[3] ZEDALIS, M., FINE, M. E. Lattice-parameter variation of Al_3(Ti, V, Zr, Hf) in Al-2 at. % (Ti, V, Zr, Hf) alloys. *Scripta Metallurgica*, 1983, vol. 17, no. 10, pp. 1247-1251.

[4] MÁLEK, P., BARTUŠKA, P., PLEŠTIL, J. Structure and properties of melt-spun Al-Zr-Ti alloys I. *Kovové mater.*, 1999, vol. 37, no.6, pp. 386-398.

[5] JONES, H. *Rapid Solidification of Metals and Alloys*. Inst. Of Metallurgists, London, 1982.

[6] SUAREZ, M., FERNANDEZ, A., MENENDEZ, J. L., TORRECILLAS, R., KESSEL, H. U., HENNICKE, J., KIRCHNER, R., KESSEL, T. Challenges and opportunities for spark plasma sintering: A key technology for a new generation of materials. In *Sintering Applications*, InTech, 2013, pp. 319-342.

[7] LUKAC, F., CHRASKA, T., MOLNAROVA, O., MALEK, P., CINERT, J. Effect of cryogenic milling on Al7075 prepared by spark plasma sintering method. In *Powder Diffraction,* 2017, pp. 1-4.

[8] NES, E., BILLDAL, H. Nonequilibrium solidification of hyper-peritectic Al-Zr alloys. *Acta Metalurgica.*, 1977, vol. 25, no.9, pp. 1031-1037.

[9] MÁLEK, P., JANEČEK, M., SMOLA, B., BARTUŠKA, P., PLEŠTIL, J. Structure and properties of rapidly solidified Al-Zr-Ti alloys. *J. Mater. Sci.*, 2000, vol. 35, no. 10, pp. 2625-2633.

[10] MÁLEK, P., JANEČEK, M., SMOLA, B. Structure and properties of melt-spun Al-Zr-Ti alloys IV. *Kovové materiály*, 2000, vol. 38, no. 3, pp. 160-177.

[11] MÁLEK, P., JANEČEK, M., BARTUŠKA, P. Structure and properties of a powder metallurgy Al-Zr-Ti alloy. *Kovové materiály*, 2002, vol. 40, no. 6, pp. 371-388.

[12] SAHIN, E., JONES, H., Extended solubility, grain refinement and age hardening in Al - 1 to 13 wt.% Zr rapidly quenched from the melt. In *Rapidly Quenched Metals II*, The Metals Soc. London, 1978, pp. 138-146.

[13] DEVARAJ, S., SANKARAN, S., KUMAR, R. Influence of spark plasma sintering temperature on the densification, microstructure and mechanical properties of Al-4.5 wt.% Cu alloy. *Acta Metall. Sin.*, 2013, vol. 26, no.6, pp. 761-771.

[14] RYUM, N. Precipitation and recrystallization in an Al-0.5 wt.% Zr-alloy. *Acta Metallurgica*, 1969, vol. 17, no. 3, pp. 269-278.

[15] KNIPLING, K. E., DUNAND, D. C, SEIDMAN, D. N. Precipitation evolution in Al-Zr and Al-Zr-Ti alloys during aging at 450-600 °C. *Acta Materialia*, 2008, vol. 56, no. 6, pp. 1182-1195.